DOE/EV/04548-1

SIMULTANEOUS BOILING AND SPREADING OF LIQUEFIED-PETROLEUM GAS ON WATER

FINAL REPORT
for Period December 12, 1978 - March 31, 1981

H. R. Chang and Robert C. Reid

Department of Chemical Engineering
Massachusetts Institute of Technology
Cambridge, MA 02139

April 1981

The U.S. Department of Energy
Agreement No. DE-AC02-77EV04548

DISCLAIMER

ABSTRACT

An experimental and theoretical investigation was carried out to study the boiling and spreading of liquid nitrogen, liquid methane and liquefied petroleum gas (LPG) on water in a one-dimensional configuration. Primary emphasis was placed on the LPG studies.

Experimental work involved the design and construction of a spill/spread/boil apparatus which permitted the measurement of spreading and local boil-off rates. With the equations of continuity and momentum transfer, a mathematical model was developed to describe the boiling-spreading phenomena of cryogens spilled on water. The model accounted for a decrease in the density of the cryogenic liquid due to bubble formation.

The boiling and spreading rates of LPG were found to be the same as those of pure propane. An LPG spill was characterized by the very rapid and violent boiling initially and highly irregular ice formation on the water surface. The measured local boil-off rates of LPG agreed reasonably well with theoretical predictions from a moving boundary heat transfer model. The spreading velocity of an LPG spill was found to be constant and determined by the size of the distributor opening. The maximum spreading distance was found to be unaffected by the spilling rate. These observations can be explained by assuming that the ice formation on the water surface controls the spreading of LPG spills. While the mathematical model did not predict the spreading front adequately, it predicted the maximum spreading distance reasonably well.

Liquefied petroleum gas (LPG) is often transported in bulk within large insulated tankers. An accidental spill of such a fluid on water could lead to a serious hazard since LPG boils well below ambient water temperature and forms a combustible (and, possibly, an explosive) cloud.

LPG consists primarily of propane with some ethane and butane. When brought in contact with water, LPG vaporizes very rapidly and forms a flammable cloud which is more dense than air and is not readily dispersed. A serious accident is conceivable if the cloud contacts an ignition source. Evaluating the potential hazards from accidents in marine transportation requires reliable data of boil-off rates and spreading rates for LPG spills on water.

Previous experimental work was limited to LPG spills on confined water surfaces. It was not known whether the evaporation rates measured in the confined area experiments were applicable to unconfined spills where boiling and spreading occur simultaneously. No experiments had been reported which determined such rates for LPG spills. It was the objective of the present work to measure experimentally the simultaneous boiling and spreading rates for LPG spilled on a water surface. A model was developed which described the boiling/spreading phenomena of LNG and LPG spills on water. Finally, a better understanding of the fundamentals and mechanism of LPG spills on water was also an important objective.

RELEVANT PREVIOUS WORK

Reid and Smith (1978) conducted spills of propane and LPG on water in an adiabatic calorimeter, placed on a load cell to record the mass of the sys-

tem continuously. For a rapid spill of propane or LPG, the initial boiling rate was found to be extremely fast and ice formation took place almost instantaneously on the water surface. Within a few seconds, the water surface was covered by a rough ice sheet, the boiling rate dropped to a smaller value, and the vaporization then could be well described by a moving boundary model (Eckert and Drake (1975)). The boiling rates of LPG were found to be the same as those of pure propane.

Very few experiments have been conducted which examine simultaneous boiling and spreading rates for any volatile cryogen. Burgess et al. (1970) used an overhead camera to study LNG spills from a point source onto an open pond. The spreading rate was reported to be constant (0.38 m/s). The boiling rate was assumed to be the same for both confined and unconfined spills and equal to 92 kW/m^2. The time (τ) required to evaporate an initial quantity V_o of LNG and the corresponding pool diameter (d_{max}) were estimated by

$$\tau = 24.9\ V_o^{1/3} \quad (V_o \text{ in } m^3,\ \tau \text{ is s}) \qquad \text{(I-1)}$$

$$d_{max} = 19.0\ V_o^{1/3}\ (m) \qquad \text{(I-2)}$$

By examining Burgess' spreading data, in general, the relationship of constant spreading rate was obeyed in the early part of the tests, but later the spreading rate decreased.

Boyle and Kneebone (1973) made three spills of LNG on a pond and measured the pool diameter when the pool began to break up into discrete patches. The spreading rate was reported to be constant during a test, but, unexpectedly, it decreased as the amount of LPG spilled increased. The thickness of LNG at pool break-up was found to be 1.8 mm. The boiling rate was calculated from the experimentally observed time for pool break-up (corresponding to the thickness of

1.8 mm) and equalled 15 kW/m^2.

Boyle and Kneebone claimed that in a spreading situation, ice did not form and boiling rates should be lower than those for confined spills.

Other studies of boiling and spreading of cryogenic liquids on water have been theoretical and based predominantly upon studies of non-volatile oil spills on water.

Hoult (1972b) coupled the evaporation and spreading rates of LNG to predict the maximum pool radius and the time for complete vaporization for LNG spilled on open water. By assuming that the heat used to evaporate LNG came from freezing of the water and neglecting the volume loss of LNG during spreading Hoult obtained the following expressions for τ (the time for complete vaporization) and r_{max} (maximum pool radius at time τ):

$$\tau = 27.8\ V_o^{1/3} \quad (V_o \text{ in } m^3, \tau \text{ in s}) \qquad \text{(I-3)}$$

$$r_{max} = 8.1\ V_o^{5/12}\ (m) \qquad \text{(I-4)}$$

In Hoult's analysis, the sensible cooling of ice and water were neglected. The only thermal resistance was within the ice layer, no surface resistance from the initial film boiling of LNG was considered.

Fay (1973) improved Hoult's model by accounting for the sensible heat of ice subcooled below the freezing temperature and obtained the following expressions for τ and r_{max} for LNG spills:

$$\tau = 9.8\ V_o^{1/3} \quad (V_o \text{ in } m^3, \tau \text{ in s}) \qquad \text{(I-5)}$$

$$r_{max} = 5.8\ V_o^{5/12}\ (m) \qquad \text{(I-6)}$$

By equating the gravitational spreading force to the inertial resistance

force, using a constant heat flux ($\dot{q}$) and mean thickness approximation, Raj and Kalelkar (1973) developed a model to predict the maximum pool radius and the time required to evaporate an initial spilled volume V_o:

$$\tau = 1.67 \left[\frac{\rho_L^2 \, \Delta H_v^2 \, V_o}{g\Delta \dot{q}^2}\right]^{1/4} \qquad \text{(I-7)}$$

$$r_{max} = \left[\frac{\rho_L^2 \, \Delta H_v^2 \, g\Delta \, V_o^3}{\dot{q}^2}\right]^{1/8} \qquad \text{(I-8)}$$

where ρ_L is the cryogen density, ΔH_v is the heat of vaporization, g is the gravitational acceleration, and Δ is the ratio of the density difference between water and cryogen to the density of water.

With $\dot{q}$ = 92 kW/m^2, for LNG:

$$\tau = 21.0 \, V_o^{1/4} \quad (V_o \text{ in } m^3, \tau \text{ in s}) \qquad \text{(I-9)}$$

$$r_{max} = 8.7 \, V_o^{3/8} \quad (m) \qquad \text{(I-10)}$$

Using the same assumptions as those for radial spreading, Raj (1977) developed a one-dimensional boiling/spreading model in which the spreading distance (x) as a function of time (t) can be expressed as follows:

$$x = 1.39 \left[\frac{g\Delta \, V_o \, t^2}{w}\right]^{1/3} + 0.097 \left[\frac{\dot{q}}{\rho_L \, \Delta H_v}\right] \left[\frac{(g\Delta)^2 \, wt^7}{V_o}\right]^{1/3} \qquad \text{(I-11)}$$

Where w is the width of spreading channel.

The time for complete vaporization (t_e) and the corresponding maximum spreading distance (x_e) are given by

$$t_e = 1.09 \left[\frac{(V_o/w)^2}{g\Delta \, (\dot{q}/\rho_L \, \Delta H_v)^3}\right]^{1/5} \qquad \text{(I-12)}$$

$$x_e = 1.59 \left[\frac{g\Delta\ (V_o/w)^3}{(\dot{q}/\rho\Delta H_v)^2} \right]^{1/5} \qquad \text{(I-13)}$$

Muscari (1974) proposed a numerical model to describe the radial spreading and boiling process for instantaneous spills of cryogens on water. He assumed the gravity force balanced the inertia of spreading fluid and the leading edge was considered as an intrusion. By assuming a constant boil-off rate, Muscari solved the conservation equations of continuity and momentum numerically and was able to predict the thickness profile of the spreading cryogen and the path of the spreading-front as well as the trailing-edge. The maximum pool radius and the time for complete vaporization for a given quantity V_o are expressed as:

$$\tau = 0.80 \left[\frac{\rho_L^{\ 2}\ \Delta H_v^{\ 2}\ V_o}{g\Delta\ \dot{q}^2} \right]^{1/4} \qquad \text{(I-14)}$$

$$r_{max} = 1.23 \left[\frac{\rho_L^{\ 2}\ \Delta H_v^{\ 2}\ g\Delta\ V_o^{\ 3}}{\dot{q}^2} \right]^{1/8} \qquad \text{(I-15)}$$

By accounting for the evaporation of cryogen during spreading, Otterman applied the radial spread law of oil spills, with the initial spilled volume divided by 2 for LNG spills. Assuming a constant heat flux, Otterman obtained the following expressions for τ and r_{max}:

$$\tau = 0.75 \left[\frac{\rho_L^{\ 2}\ \Delta H_v^{\ 2}\ V_o}{g\Delta\ \dot{q}^2} \right]^{1/4} \qquad \text{(I-16)}$$

$$r_{max} = 0.82 \left[\frac{\rho_L^{\ 2}\ \Delta H_v^{\ 2}\ g\Delta\ V_o^{\ 3}}{\dot{q}^2} \right]^{1/8} \qquad \text{(I-17)}$$

In Table I-1, the predicted values of τ and r_{max} from these various models are compared with the experimental data of Boyle and Kneebone. Note the poor

TABLE I-1

Boyle's Data Compared with Predictions from Various Models
For LNG Spills in a Radial Configuration

Spill Size, $2.24 \times 10^{-2} m^3$	Boyle (Experimental)	Burgess	Hoult	Fay	Muscari	Raj	Otterman
Pool Diameter at Break up, m	3.96	5.36	3.33	2.38	5.14	4.18	3.42
Time to Evaporate Completely, s	24.	7.0	7.8	2.5	9.8	8.1	11.6
Spill Size, $4.48 \times 10^{-2} m^3$							
Pool Diameter at Break-up, m	5.64	6.75	4.44	3.18	6.68	5.43	4.43
Time to Evaporate Completely, s	33.	8.8	9.9	3.1	11.6	9.7	13.8
Spill Size, $8.97 \times 10^{-2} m^3$							
Pool Diameter at Break up, m	7.32	8.5	5.93	4.25	8.66	7.04	5.75
Time to Evaporate Completely, s	35.	11.1	12.4	3.9	13.8	11.5	16.4

agreement for different analyses. Fay's model gives much smaller value of τ and r_{max} than those predicted by the others. This is because in his analysis, Fay assumed that the energy to evaporate LNG comes from freezing of the water and the sensible heat released as ice cools below its freezing point. He also neglected the surface resistance to boiling due to the initial vapor film formation at the LNG-water interface and the resulting lower heat transfer rate. The maximum pool diameters predicted on the basis of Raj and Kalelkar's model are in good agreement with Boyle's data. The values of τ predicted from the models mentioned above are much lower than experimental results. This is not unexpected because all the models (except Muscari's) assume that the circular area uniformly covered with LNG continues to increase as long as any liquid cryogen remains. However, Boyle and Kneebone observed that the LNG pools broke up into discontinuous areas before complete vaporization. Using a "continuous pool" assumption for the LNG layer therefore results in underestimating the time for complete vaporization because the cryogen-water contact area is overestimated.

In summary, few experiments have been conducted to examine the simultaneous boiling and spreading of LNG on water. The available data do not agree well with the theories that have been proposed. For LPG, essentially no research had been done to describe the boiling and spreading phenomena following a spill on water.

EXPERIMENTAL

The experimental apparatus was designed for the study of the boiling and spreading of cryogenic liquids spilled on water in a one-dimensional configuration. A schematic representation of the apparatus is given in Figure I-1. The equipment consists of six major parts: (1) the liquefaction station, (2) the cryogen distributor, (d) a water trough, (4) the vapor sampling stations, (5)

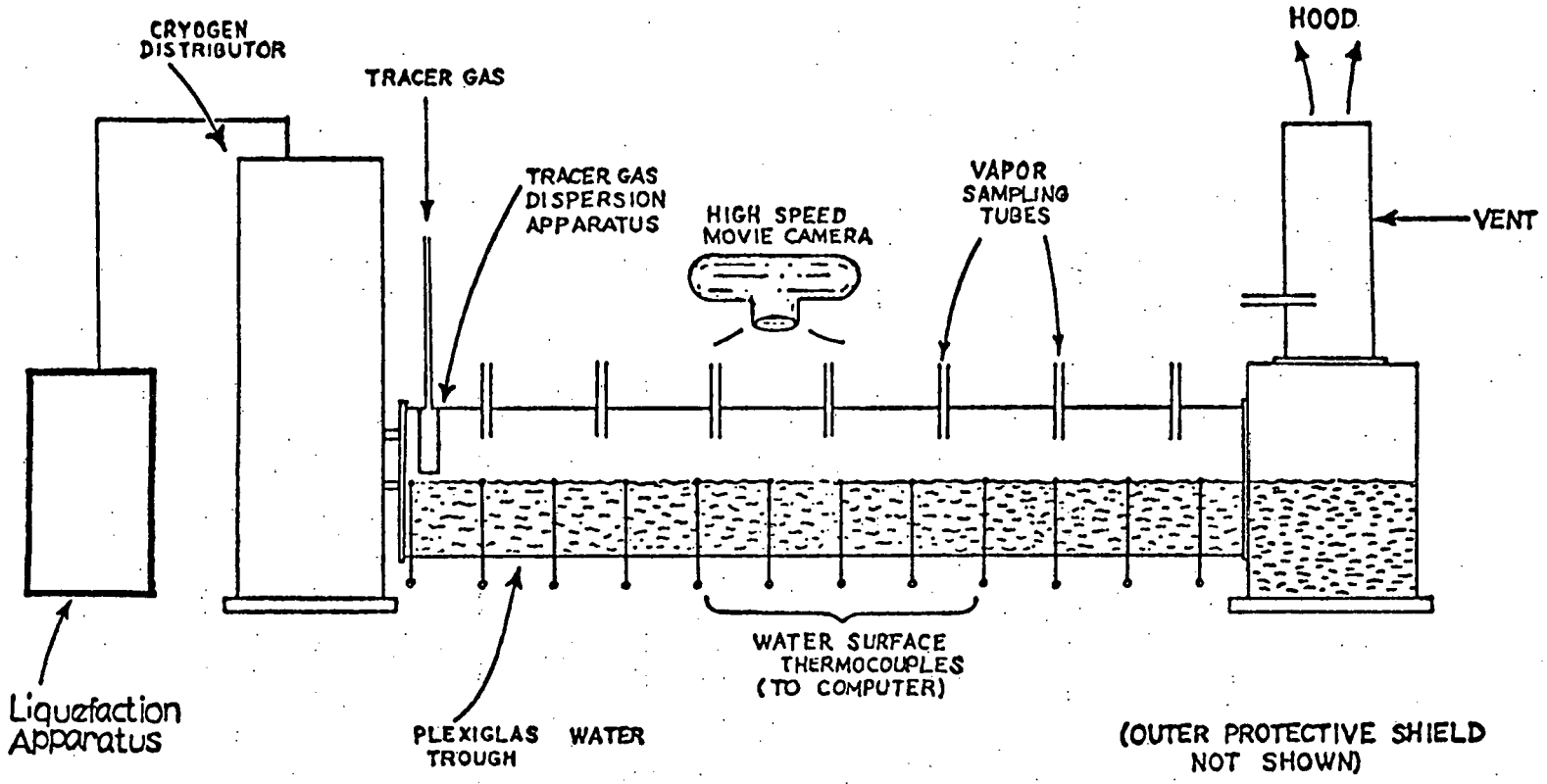

FIGURE I-1: SCHEMATIC OF SPILL/SPREAD/BOIL APPARATUS

the hood connection, and (6) a safety shield.

The cryogenic liquids were prepared in the liquefaction station by cooling the cryogen gases below their boiling points with liquid nitrogen. After a sufficient quantity has been prepared, as indicated by the weight change of the gas cylinder, the cryogen liquid was delivered from the liquefaction station to the cryogen distributor by pressurizing the liquefaction station with helium gas.

The cryogen distributor employs a spring-loaded piston which, upon release, will open a side port through which the cryogen can be delivered rapidly onto the water surface without severe disruption of the water surface. A programmable sequencer was used to release the distributor piston at a pre-selected time. The distributor was fabricated from Lexan polycarbonate resin to permit visual observation of the cryogen level. The dimensions of the distributor are 17.8 cm O.D. x ~ 60 cm in height. The maximum liquid capacity of the distributor is ~ 3 liters. Upon full downward displacement of the piston, the effective cross-sectional flow area through the side port is ~ 48 cm^2.

The simultaneous boiling and spreading experiments were conducted in a long, narrow water trough. The trough consisted of Plexiglas tubing and was half filled with water. A set of liquid-thermocouples placed on the water surface indicated the passage of the cryogen. Vapor temperatures were monitored by a set of vapor-thermocouples introduced through the top of the spill tube. The thermocouple out-puts were fed directly into a NOVA-840 Real Time Computer.

The local boil-off rates of cryogen spreading on water were estimated in an indirect manner. A tracer gas, CO_2, was injected continuously and evenly at steady state into the system through a gas dispersion apparatus. Vapor samples were collected at several locations along the water trough during the experiment. A gas chromatograph was used to analyze the vapor samples. The temperatures and compositions of vapor samples provided the necessary informa-

tion to determine the mass boiled off as a function of time and position.

Eight sampling stations were used to collect vapor samples at specified times during the experiment; each sampling station was able to collect six different samples. Figure I-2, is a transverse view of one sample station. The sampling bulbs were initially purged and pressurized with argon gas. The operation of the sample intake was controlled automatically by the sequencer.

The envolved cryogen vapor and tracer gas were ducted to the hood.

A high speed carmera was used to record the movement of the cryogen over the water surface.

DATA ANALYSIS TO DETERMINE LOCAL BOIL-OFF RATES

The differential mass balances for tracer gas and hydrocarbon cryogen vapor can be expressed as follows:

$$\frac{\partial C_T}{\partial t} = - \frac{\partial (UC_T)}{\partial x} \qquad \text{(I-18)}$$

$$\frac{\partial C_{HC}}{\partial t} = - \frac{\partial (UC_{HC})}{\partial x} + \left(\frac{w}{A}\right) \dot{M} \qquad \text{(I-19)}$$

where C_T and C_{HC} are the molar concentrations of tracer gas and cryogen vapor respectively. U is the vapor velocity. $\dot{M}$ is the local mass boil-off rate (moles per unit area). w is the width of the water trough.

Vapor temperature measurements were used to calculate the molar density (C) of the vapor with the equation of state:

$$C = \frac{P}{ZRT} \qquad \text{(I-20)}$$

where P = pressure, 1 bar

Z = compressibility factor

R = universal gas constant, 83.14 bar-cm^3/mol-K

T = vapor temperature, K

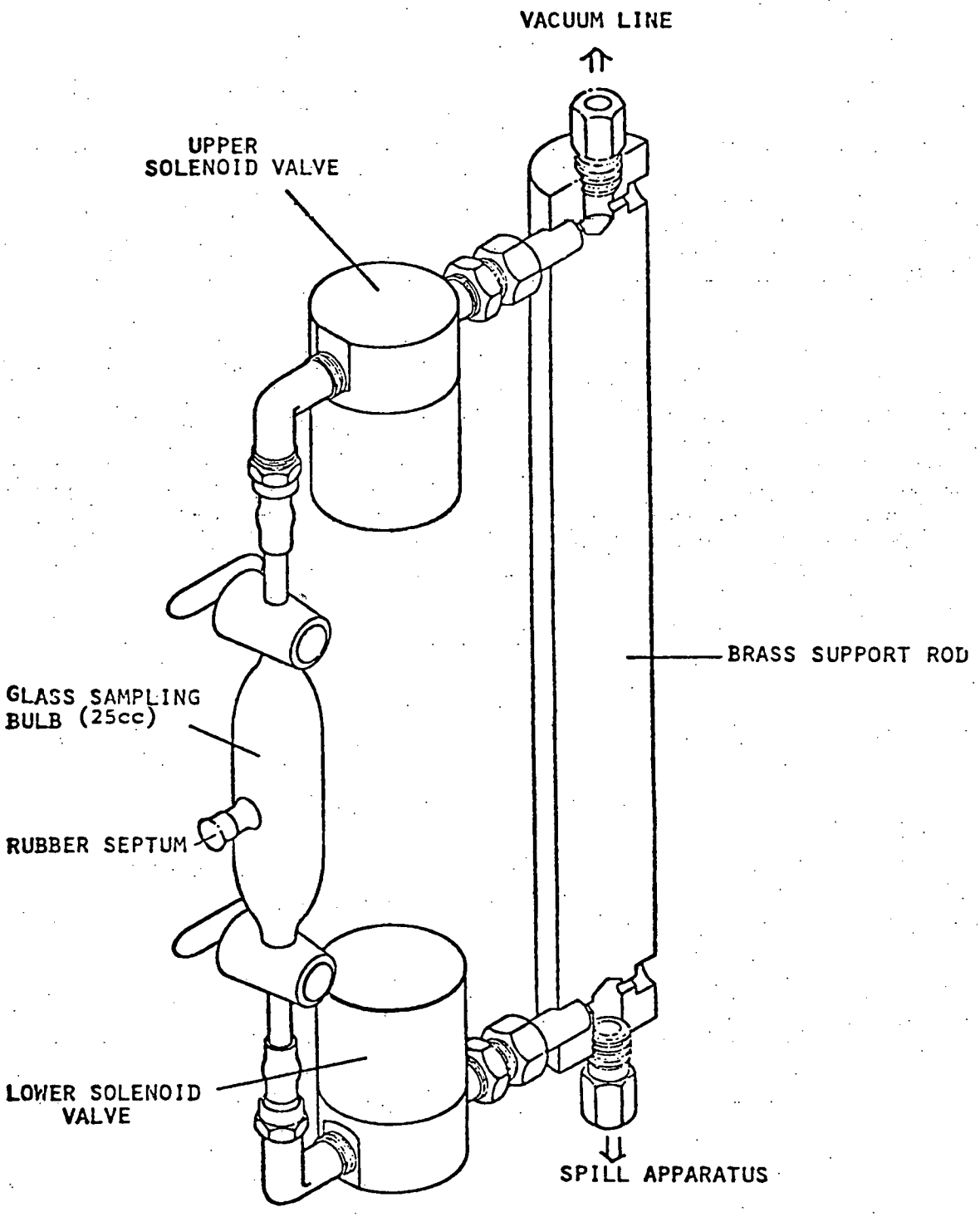

FIGURE I-2: ISOMETRIC CUT-AWAY VIEW OF VAPOR SAMPLING STATION

The concentrations of tracer gas (C_T) and cryogen vapor (C_{HC}) were estimated by vapor sample analyses:

$$C_T = x_T \cdot C \tag{I-21}$$

$$C_{HC} = C - C_T \tag{I-22}$$

where x_T = mole fraction of the tracer gas.

A numerical finite difference technique was used to evaluate the gas velocity (U) and local boil-off rates ($\dot{M}$).

$$\frac{(C_T)_{i+1,\,j} - (C_T)_{i,\,j}}{t_{i+1} - t_i} = -\left[\frac{(UC_T)_{i+1,\,j} - (UC_T)_{i+1,\,j-1}}{x_j - x_{j-i}}\right] \tag{I-23}$$

$$\frac{(C_{HC})_{i+1,\,j} - (C_{HC})_{i,\,j}}{t_{i+1} - t_i} = -\left[\frac{(UC_{HC})_{i+1,\,j} - (UC_{HC})_{i+1,\,j-1}}{x_j - x_{j-1}}\right] + \left(\frac{w}{A}\right) \dot{M}_{i+1,j} \tag{I-24}$$

i is the ith time interval and j is the jth space interval. $\dot{M}_{i+1,\,j}$ is the local mass boil-off rate at jth spatial point and (i+1)th instant in time.

The algorithm began with the known velocity at j = 0 (x=0). Equation (I-23) was used to solve for the gas velocity $U_{i+1,\,j}$, which was then substituted into equation (I-24) to yield the local boil-off rate $M_{i+j,\,j}$.

ONE-DIMENSIONAL BOILING/SPREADING MODEL FOR INSTANTANEOUS SPILLS OF CRYOGENIC LIQUIDS ON WATER

The spreading mechanics of cryogenic liquids on water is similar in many respects to that of non-volatile liquids on water. The major distinction between these two processes is the evaporative mass loss of cryogen during the spreading.

Fay (1969) used an order-of-magnitude analysis to identify three principle flow regimes through which a spreading oil film passes: the first is the grav-

ity-inertia regime, the second is the gravity-viscous regime and the third is the surface tension-viscous regime. For cryogen spilled on water, only the physics of the first regime is important. Before the second or third regime becomes established, most of the cryogen has evaporated.

Assuming the density of the cryogen (ρ) is constant and the cryogen is in hydrostatic equilibrium in the vertical direction, neglecting the acceleration across the thickness (h) of the cryogen layer, the equations of continuity and momentum transfer in one-dimensional configuration can be expressed as:

$$\frac{\partial h}{\partial t} + \frac{\partial}{\partial x}(hU) + \frac{\dot{m}}{\rho} = 0 \qquad \text{(I-25)}$$

$$\frac{\partial U}{\partial t} + U\frac{\partial U}{\partial x} + \Delta g \frac{\partial h}{\partial x} = 0 \qquad \text{(I-26)}$$

where x is the spreading direction and t is time. U is the spreading velocity and $\dot{m}$ is the local mass boil-off rate per unit area (it can be a function of both x and t). Δ is defined as $(\rho_{water} - \rho)/\rho_{water}$ and g is the gravitational acceleration.

The boundary conditions are:

at the leading edge: $$U_{LE} = [\lambda \Delta g\, h_{LE}]^{1/2} \qquad \text{(I-27)}$$

at the origin of the spill: $$U_{x=0} = 0 \qquad \text{(I-28)}$$

where λ is experimentally determined and equal to 1.64.

The initial condition is evaluated at a time very close to the start of the spill when the amount of cryogen evaporated is very small so that the spill process can be adequately described by Hoult's (1972a) analytical solution for oil spills on water, which is expressed as:

$$x = \eta \left[\frac{g\Delta V t^2}{W}\right]^{1/3} \qquad \text{(I-29)}$$

where

$$\eta = \left[\frac{4}{9\lambda} - \frac{2}{27}\right]^{-1/3} \qquad \text{(I-30)}$$

A numerical technique called "the method of characteristics" was used to solve equations (I-25) and (I-26) and U and h as functions of x and t were determined.

For the case of constant boil-off rate (per unit area), the theoretical thickness profile of the spreading fluid (in dimensionless form) is shown in Figure I-3; the spreading front is thicker and the tail thins out towards the spill origin. As the cryogen continues to evaporate, a trailing edge begins to appear at x = 0 and moves toward the spreading front. The numerical model predicts the paths of the leading-edge and trailing-edge, as shown in Figure I-4. The intersection of these two paths determines the time for complete vaporization and the maximum spreading distance.

As a cryogenic liquid spills on an unconfined water surface, boiling and spreading occur simultaneously. The bubbles of the evaporated cryogen rising through the liquid reduce the effective density of liquid cryogen layer. The reduction in density can be estimated using the average bubble rising velocity (U_{av}) and volumetric flux ($\dot{V}$):

$$\rho_{effective} = \rho_L \left(1 - \frac{\dot{V}}{U_{av}}\right) \qquad \text{(I-31)}$$

The bubble rising velocity is a function of the bubble size. For nitrogen and methane, the average bubble rising velocity was estimated to be 24 cm/sec. In the case of propane, U_{av} was estimated to be 26 cm/sec.

EXPERIMENTAL RESULTS

Spills of n-pentane were made and the spreading front was recorded as a

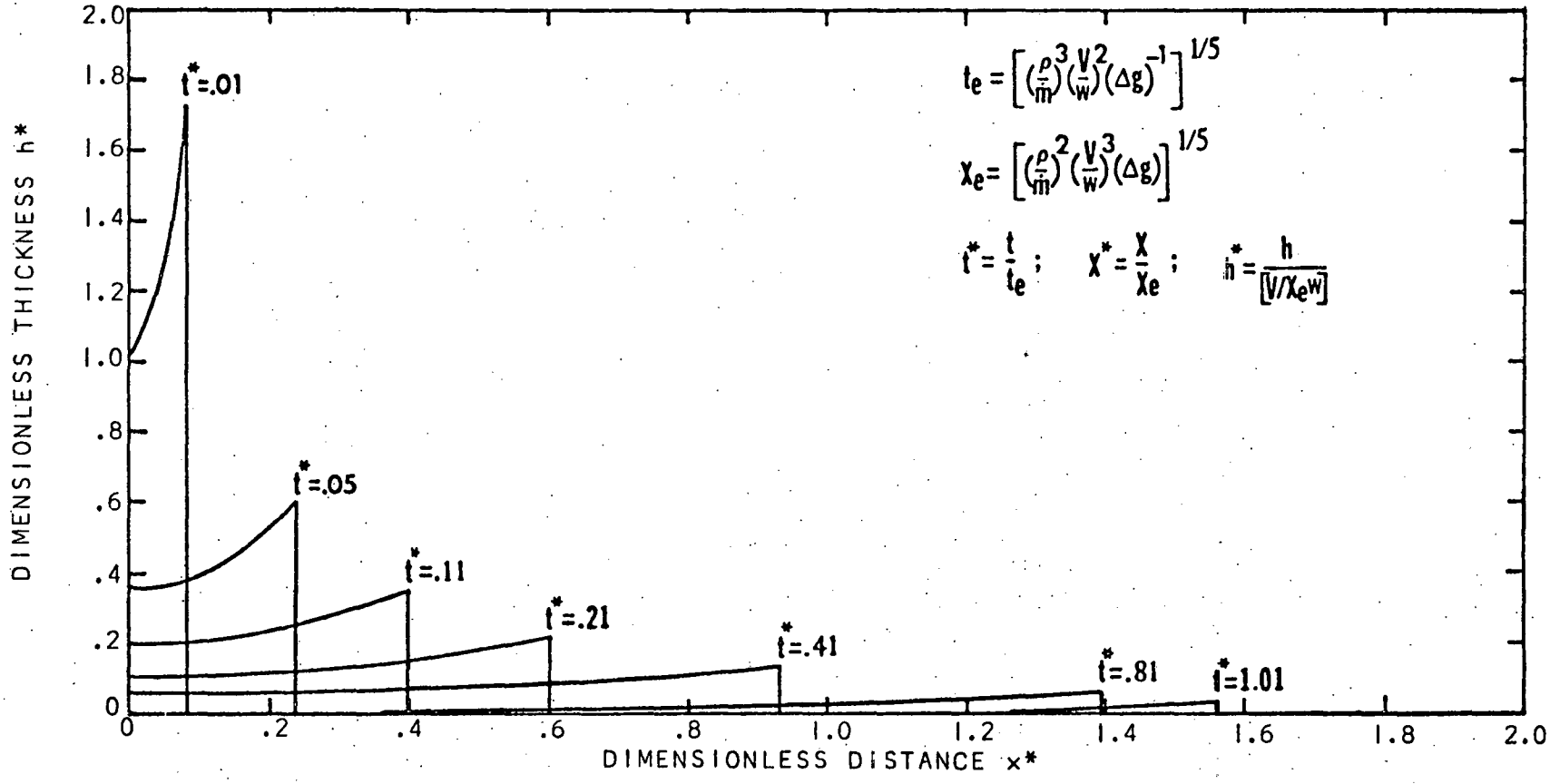

FIGURE 1-3: DIMENSIONLESS THICKNESS PROFILE PREDICTED BY THE NUMERICAL MODEL FOR THE CASE OF CONSTANT HEAT FLUX.

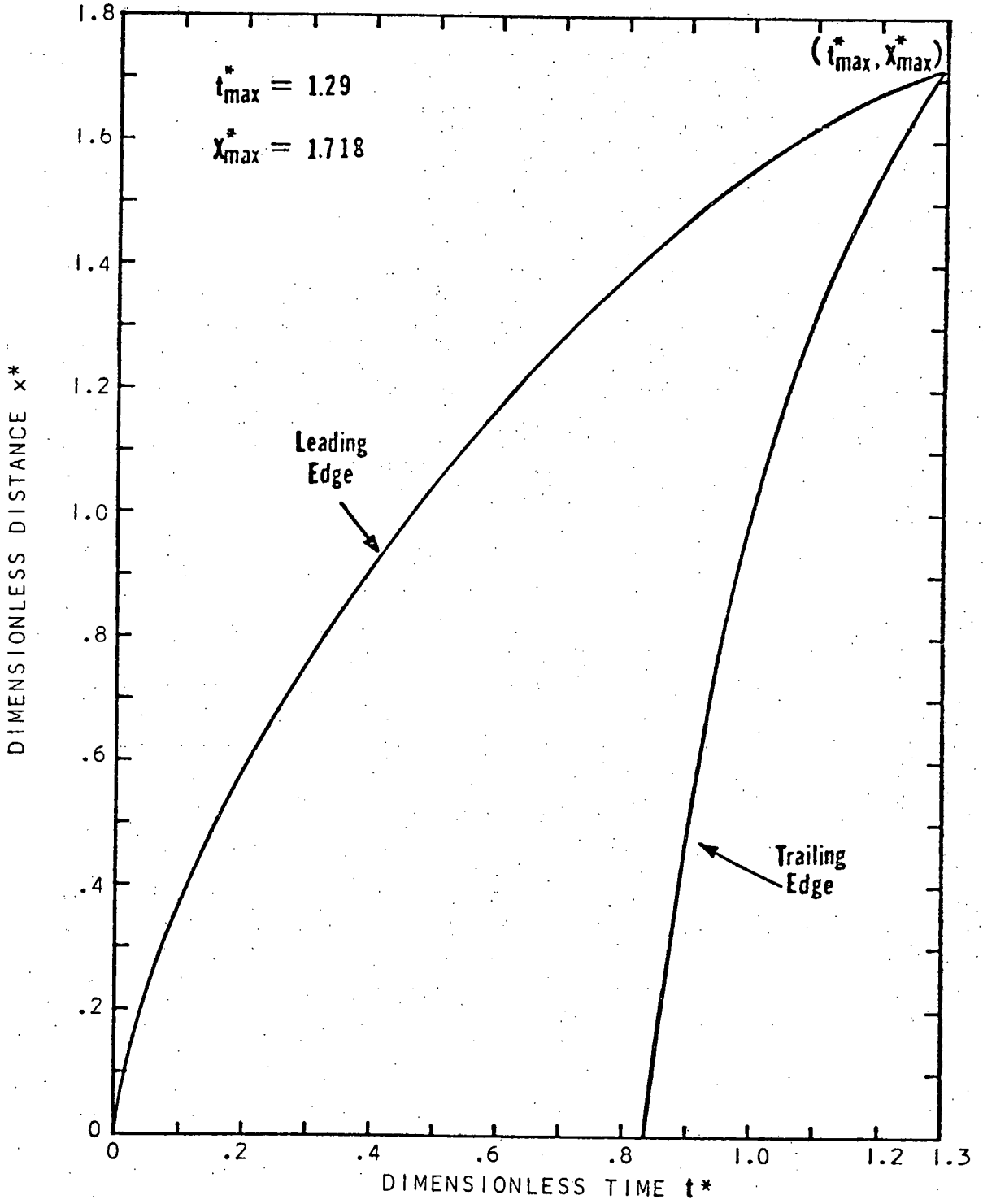

FIGURE 1-4: PATHS OF THE LEADING AND TRAILING EDGES PREDICTED BY THE NUMERICAL MODEL FOR THE CASE OF CONSTANT HEAT FLUX.

function of time. Similarly, spills were carried out with liquid nitrogen and methane. Pure liquid propane, binary mixtures of ethane-propane and propane-n-butane, and ternary mixtures of ethane-propane-n-butane were spilled on water and the spreading rates and local boil-off rates were measured.

Pentane Spills

Several pentane spill experiments were conducted to determine the value of λ in the leading-edge boundary condition (equation (I-27)). Figure I-5 presents the experimental results for pentane spills of various volumes. The value of n in equation (I-29) was found to be 1.72. λ was then obtained from equation (I-30) and equalled 1.64.

Nitrogen and Methane Spills

The spreading curves for liquid nitrogen and methane as functions of time are shown in Figure I-6. During the spreading of nitrogen or methane, the cryogen is thicker near the leading edge and becomes thinner in the tail. This general shape persists until almost the end of the spreading process when most of the cryogen has evaporated. A layer of ice forms on the water surface downstream of the cryogen distributor during the experiment. In the vicinity of the cryogen distributor, no ice formation was observed.

Propane Spills

Propane boils very rapidly from its initial contact with water. Highly irregular ice forms quickly (~ 1 s). The boiling rate then drops to considerably lower values. This can be seen in Figures I-7 and I-8, where triangles represent data from a pure propane spill. The spreading distance as a function of time is shown in Figure I-9; the discontinuity is due to an "ice dam" formation, which hinders the spreading of cryogen. For the same volume spilled, the maximum spreading distance for propane is much smaller than for nitrogen or methane.

LPG Spills

The spreading data of ethane-propane, propane-n- butane, and ethane-propane-

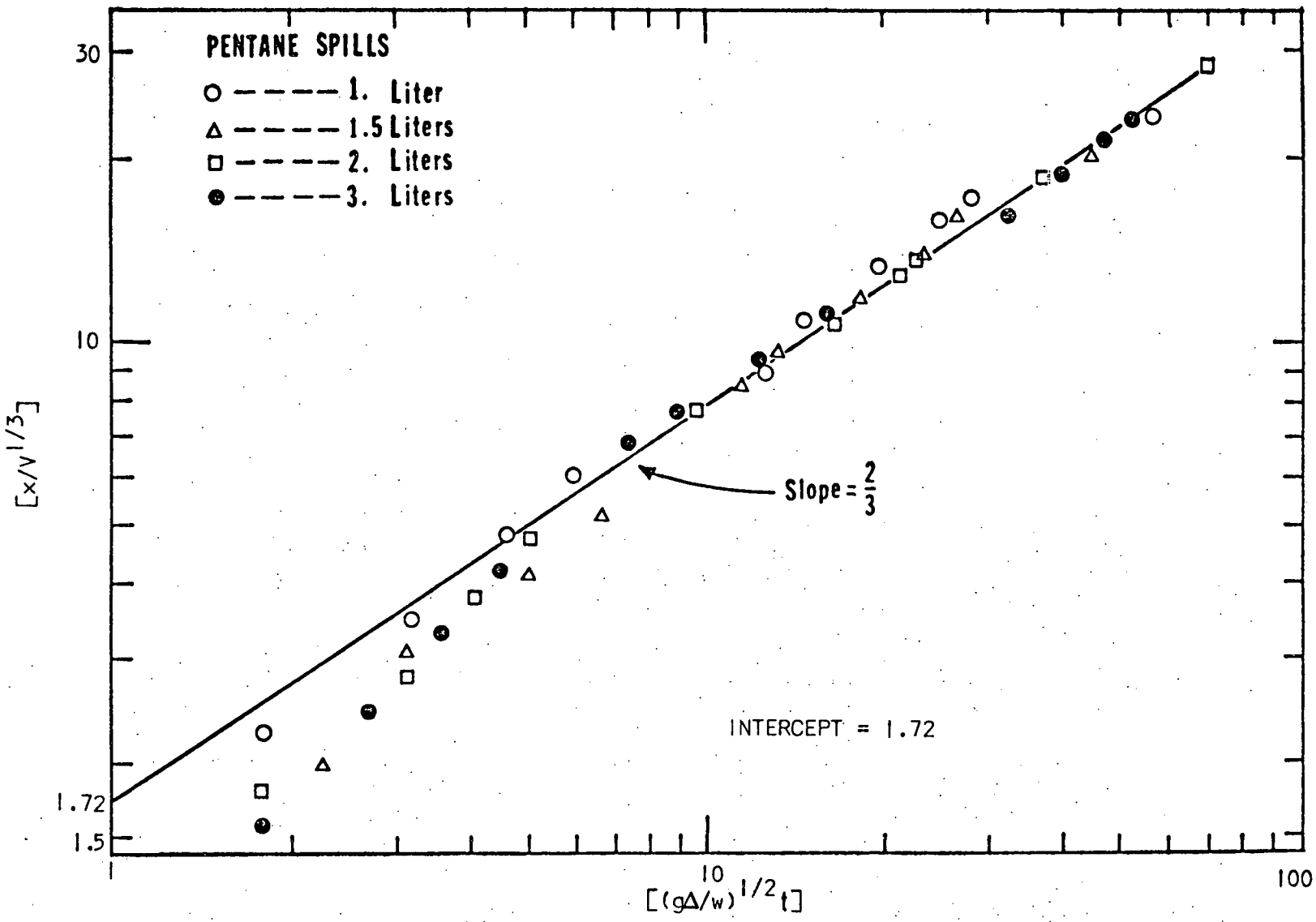

FIGURE 1-5: DIMENSIONLESS CORRELATION OF SPREADING DISTANCE WITH TIME FOR PENTANE SPILLS.

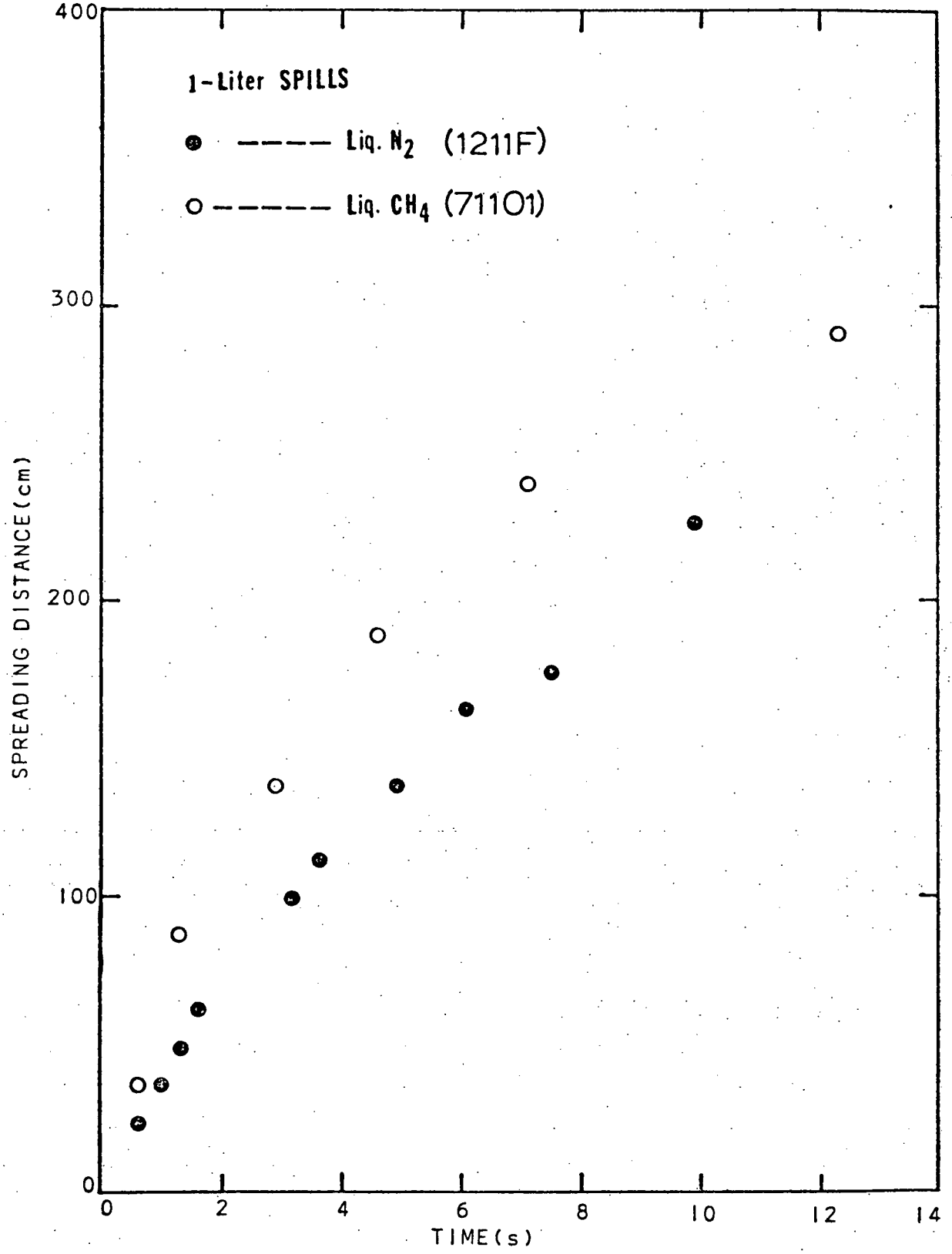

FIGURE I-6: SPREADING DISTANCE AS A FUNCTION OF TIME FOR LIQUID NITROGEN AND METHANE SPILLS

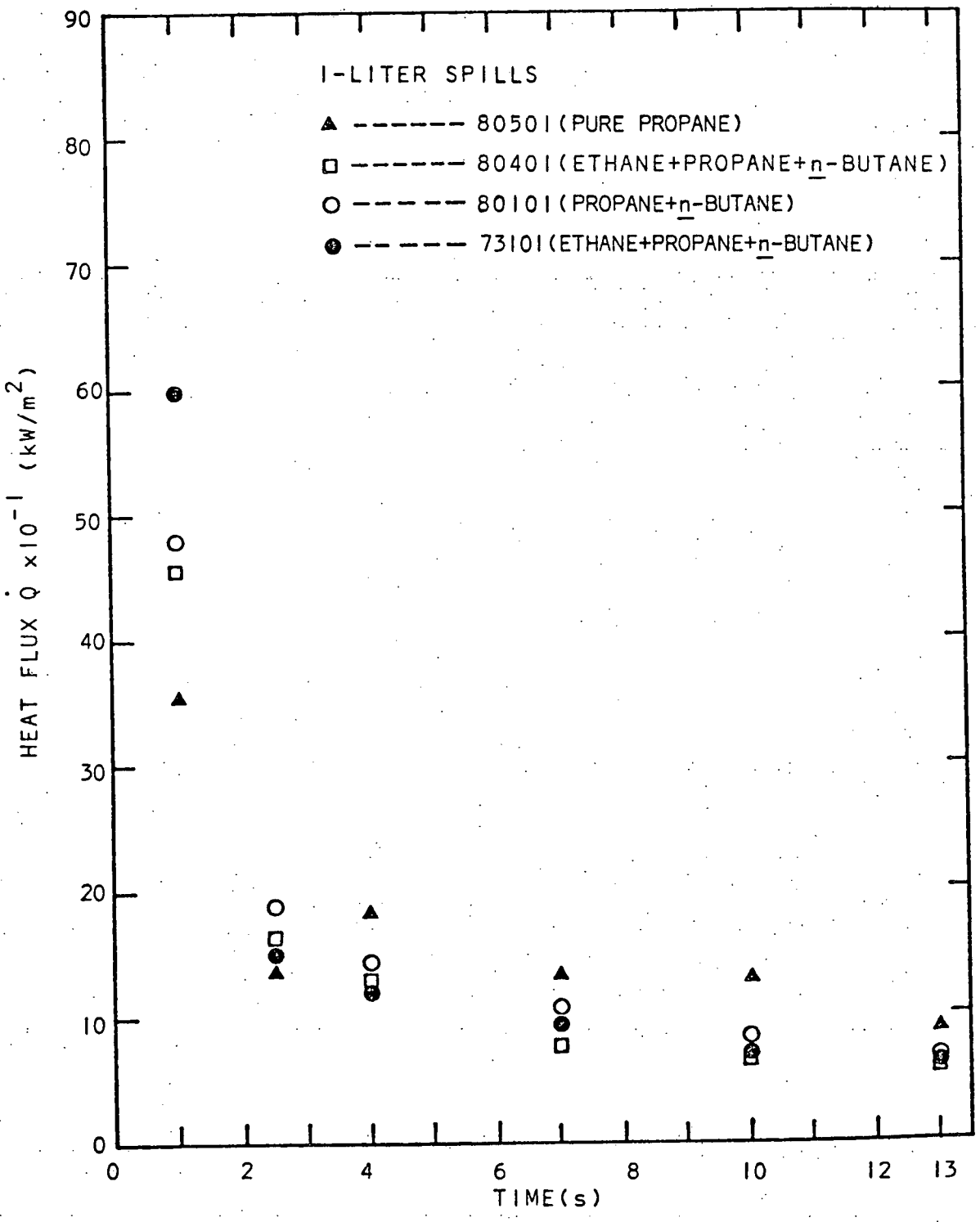

FIGURE 1-7: LOCAL BOIL-OFF RATE AS A FUNCTION OF TIME FOR PROPANE AND LPG SPILLS AT THE FIRST SAMPLING STATION.

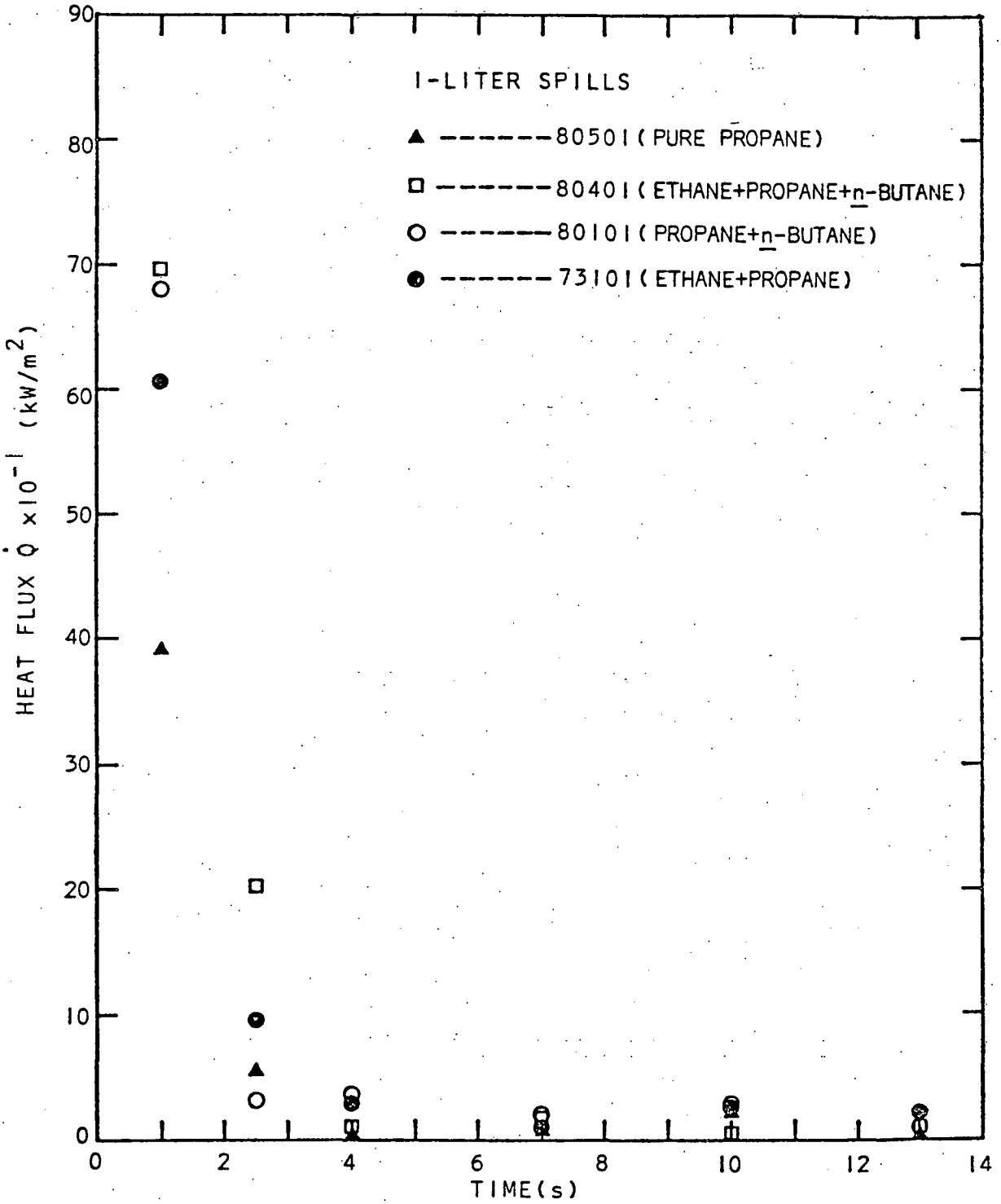

FIGURE 1-8: LOCAL BOIL-OFF RATE AS A FUNCTION OF TIME FOR PROPANE AND LPG SPILLS AT THE SECOND SAMPLING STATION.

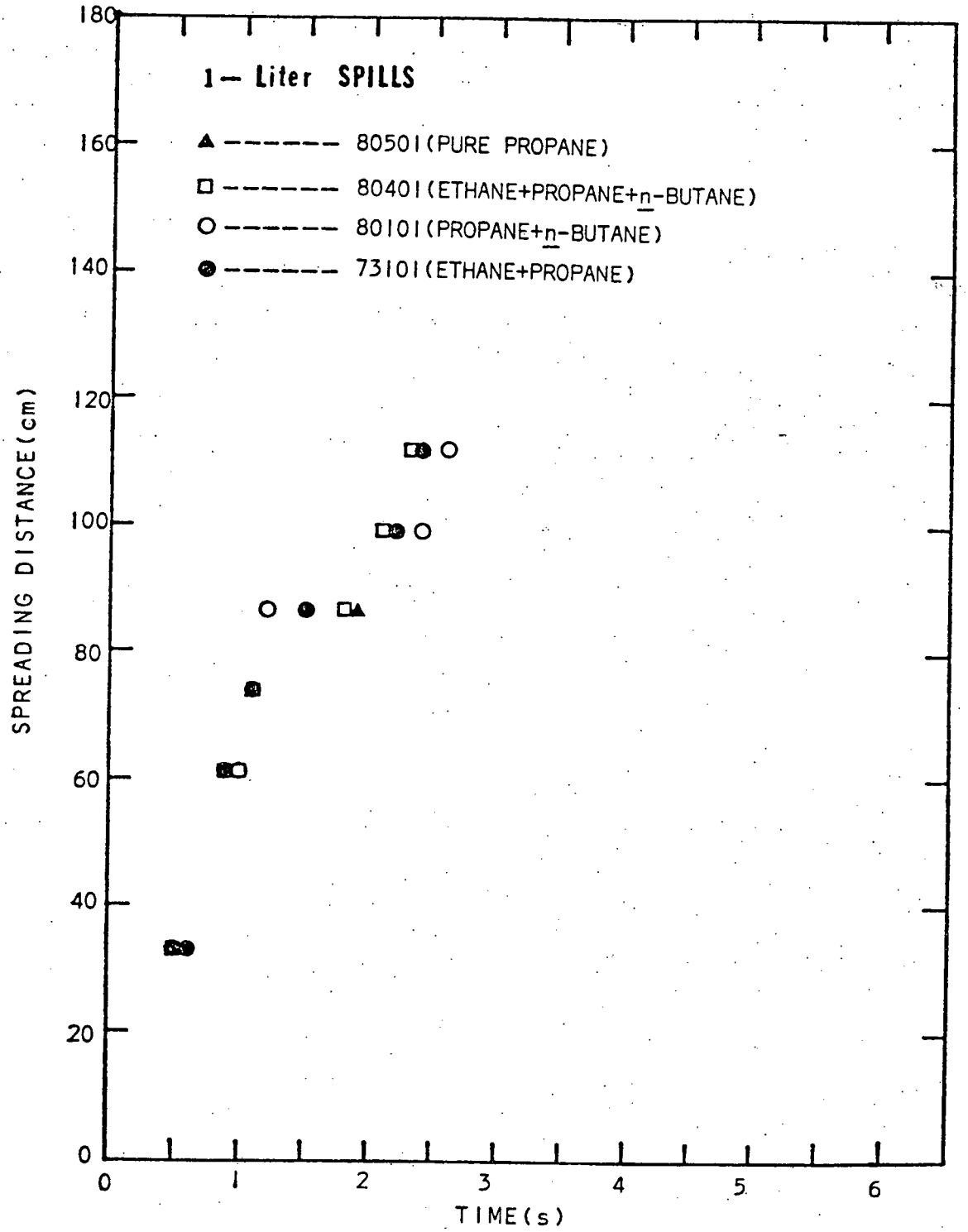

FIGURE 1-9: SPREADING DISTANCE AS A FUNCTION OF TIME FOR PROPANE AND LPG SPILLS.

n-butane mixtures are also presented in Figure I-9. In Figures I-7 and I-8, the boil-off rates for the mixtures are similar to the case of pure propane, the initial boil-off rate being very high and then decreasing very rapidly. The ice forms very quickly and is rough and irregular.

DISCUSSION

Nitrogen and Methane Spills

In Figure I-10, the experimental spreading data for liquid nitrogen and methane spills are compared to the values predicted by the numerical model described earlier. The boil-off rates of nitrogen and methane are assumed constant and selected to be 40 and 92 kW/m^2 respectively. The effective densities of nitrogen and methane are then calculated using equation (I-31) and equal to 0.66 and 0.254 g/cm^3 respectively (the normal densities of liquid nitrogen and methane at their boiling points, 77K and 111K, are 0.8 and 0.425 g/cm^3). These effective densities are used in the numerical analysis. Good agreement is obtained between the experimental data and the predicted values. For nitrogen and methane spreading on water, the leading-edge is thicker than the tail. This is consistent with theoretical predictions (see Figure I-3). The model also predicts the trailing edge where the cryogen has completely evaporated and the water surface is cryogen free. The trailing edge starts at the distributor and moves towards spreading front. The intersection of the leading edge and trailing edge determines the maximum spreading distance and the time for complete vaporization. The numerical model gives reasonable predictions of the maximum spreading distance for nitrogen and methane spills, as shown in Table I-2.

The close agreement between the experimental data and the predicted values, using an assumed constant heat flux for nitrogen or methane, proves the validity of the assumption. It is concluded that the numerical model successfully de-

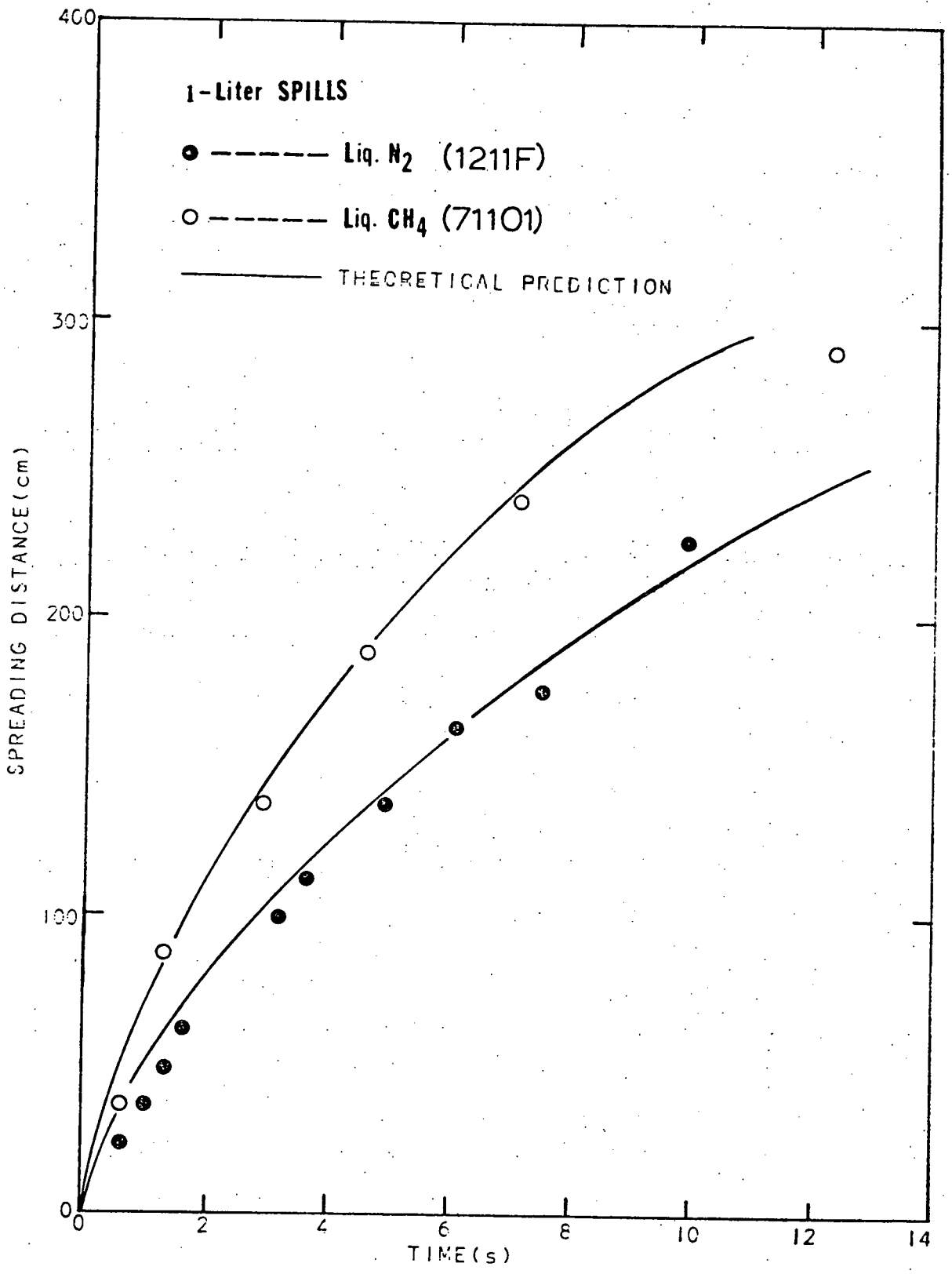

FIGURE I-10: SPREADING CURVES FOR LIQUID NITROGEN AND METHANE SPILLS. EXPERIMENTAL DATA AND NUMERICAL PREDICTIONS COMPARED.

TABLE I-2

Maximum Spreading Distance for Liquid Nitrogen and Methane Spills

Volume Spilled	Maximum Spreading Distance (cm) Nitrogen Experiment	Nitrogen Theory	Maximum Spreading Distance (cm) Methane Experiment	Methane Theory
0.5 liter	226	193	229	197
0.75 liter	---	246	279	251
1.0 liter	310	293	317	298
1.5 liters	*	374	*	380
2.0 liters	*	444	*	452

* The length of the spill apparatus is 360 cm.

scribes the boiling and spreading phenomena for nitrogen and methane spills on water (at least for this size spill).

Propane and LPG Spills

For propane or LPG spills on water, violent and rapid boiling occurs immediately upon contact. The water surface near the distributor opening is severely agitated. It is very difficult to define the true area of contact between cryogen and water at this point. Rough ice forms on the water surface very quickly (~ 1 s). From this point, heat transfer is controlled by the conduction through the ice and water; the boiling rate decreases further with time as the ice layer grows thicker. The local boiling behavior can then be reasonably well described by a moving boundary heat transfer model (Eckert and Drake (1975)). This model leads to the conclusion that the local heat flux is inversely proportional to the square root of the corrected time, t_{c_i}:

$$\dot{Q}_i = \varepsilon \, t_{c_i}^{-1/2} = 154 \, t_{c_i}^{-1/2} \ (kW/m^2) \qquad (I\text{-}32)$$

where t_{c_i} is defined as :

$$t_{c_i} = t_i - t_\delta \qquad (s)$$

ε is a function of the physical properties of ice and is evaluated at an average temperature between the freezing point of water and the boiling point of LPG. t_δ represents the time associated with the initial ill-defined boiling phase before the formation of an ice layer. The value of t_δ has been chosen equal to one second but numerical tests have shown that variations in t_δ (0.5 - 1.5 sec) do not affect the predicted results. t_i is the time ellapsed after the initial contact of water with cryogen at a position x_i where the heat flux is $\dot{Q}_i$.

Predictions from equation (I-32) are compared with experimental data in

Figures I-11 and I-12. Theory and experiment agree reasonably well for the first sampling station. The values of the heat flux obtained from the second station are below the predicted values. The explanation for this is that propane or LPG initially evaporates very fast and there is not enough cryogen to cover evenly the entire surface area between the first and second sampling stations ($\dot{Q}$ estimated by the data analysis scheme is the average heat flux between the sampling stations).

Figures I-11 and I-12 also show that the addition of small amounts of ethane and (or) n-butane to propane has no effect on its boiling rates. This is the same as the conclusion obtained from LPG spills on confined water surfaces.

The numerical model mentioned earlier can also be used to simulate the boiling-spreading process for LPG, assuming a boiling rate that changes with time according to the following equation:

$$\dot{Q}_i = \varepsilon_o \qquad 0 \leq t_i \leq 1.0 \text{ s}$$

$$\dot{Q}_i = \varepsilon \, (t_i - t_o)^{-1/2} \qquad t_i > 1.0 \text{ s} \tag{I-33}$$

where $\dot{Q}_i$ is in kW/m^2 and

$$t_o = t_\delta - \left(\frac{\varepsilon}{\varepsilon_o}\right)^2 \quad (s)$$

Equation (I-33)attempts to account for the high evaporation rate ε_o, observed in the first second of contact between water and cryogen; the value of ε_o is selected to be 10^3 kW/m^2 which is about the same as the average value of the heat fluxes obtained from various propane and LPG spills at the first second after LPG contacts the water surface.

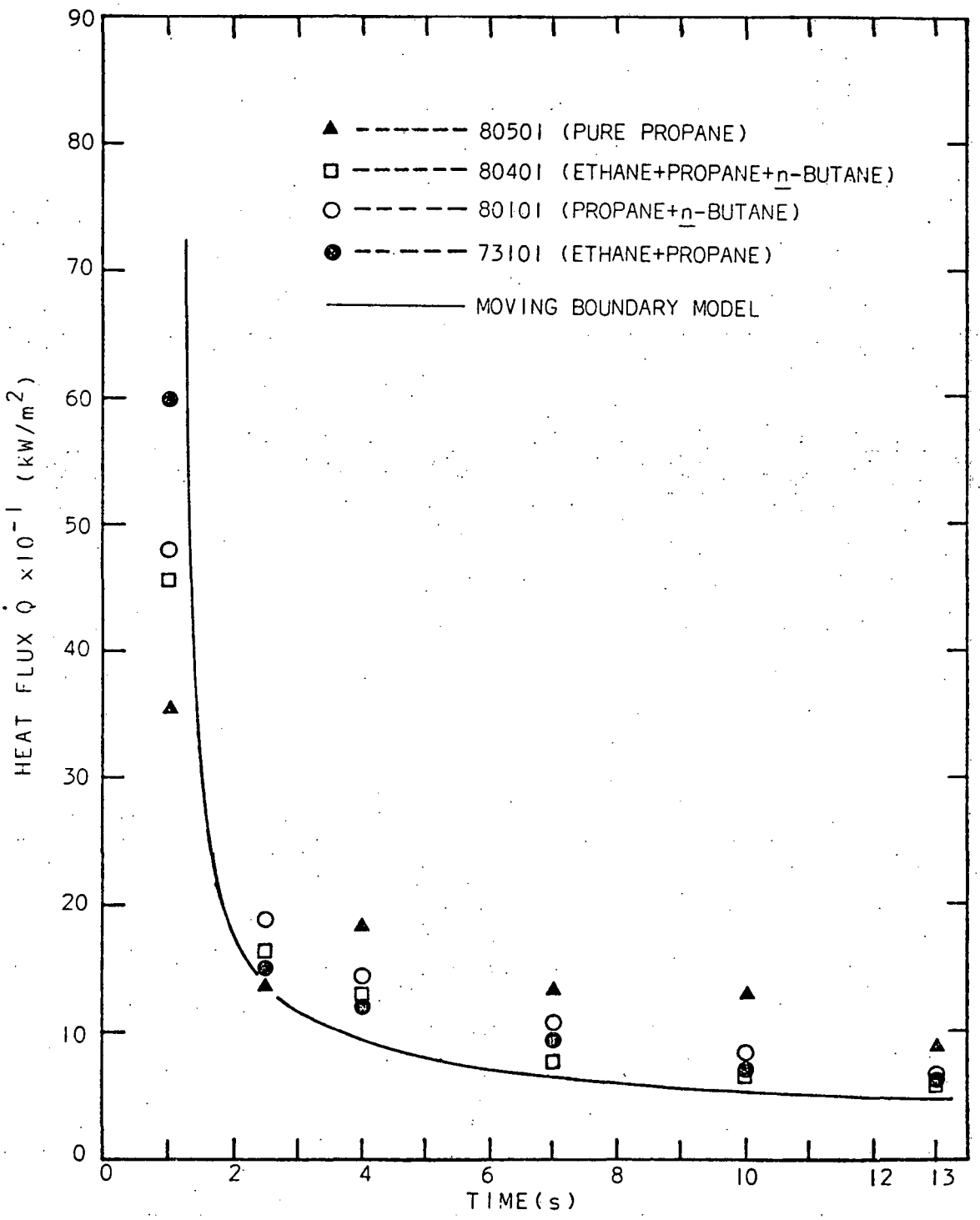

FIGURE I-11: LOCAL BOIL-OFF RATE CURVES FOR PROPANE AND LPG SPILLS AT THE FIRST SAMPLING STATION. EXPERIMENTAL DATA COMPARED WITH PREDICTIONS FROM MOVING BOUNDARY MODEL.

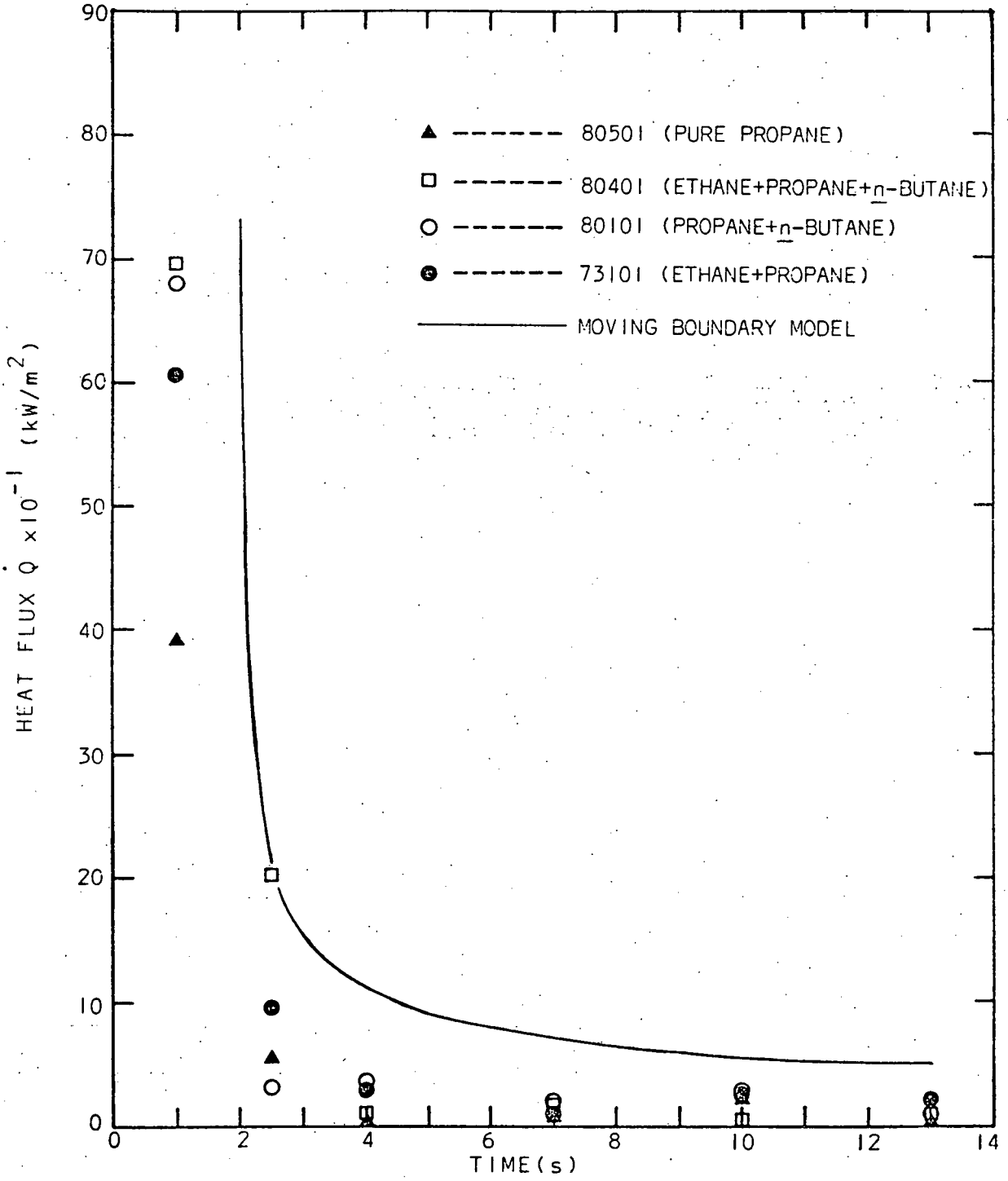

FIGURE I-12: LOCAL BOIL-OFF RATE CURVES FOR PROPANE AND LPG SPILLS AT THE SECOND SAMPLING STATION. EXPERIMENTAL DATA COMPARED WITH PREDICTIONS FROM MOVING BOUNDARY MODEL.

The effective density of LPG is set equal to 0.3 g/cm^3, using an average evaporation rate (per unit area) for the first 13 seconds after LPG contacts water and an average bubble rising velocity, 26 cm/s.

The predicted spreading curve as a function of time is compared to the experimental data in Figure I-13. The model does not accurately predict the spreading front position. The highly irregular ice formed in LPG spills is very difficult to characterize, and its effect on hindering the spreading of cryogen cannot be adequately accounted for in the theory. Figure I-13 also shows that the composition of LPG has little effect on its spreading process. Therefore, it is concluded that the boiling-spreading process for LPG spills is independent of its composition.

The predicted values of the maximum spreading distance and the experimental data are given in Table I-3. Close agreement is observed.

In Table I-4, maximum spreading distances for methane and propane spills are compared; methane spreads over a much larger area than propane (LPG) for the same volume spilled.

CONCLUSIONS

1. An apparatus was designed and constructed to monitor the spreading of a boiling liquid on water. The apparatus allows measurement of vapor temperatures and compositions. These data can be used to infer liquid vaporization rates.

2. For liquid nitrogen and methane spills, film boiling occurs initially upon contact with water. Ice forms on the water surface during the spreading. Before an ice layer appears, most of the cryogen was evaporated. Because there is little ice growth before most of the liquid nitrogen or methane has evaporated, their boiling rates were found to be nearly constant. This conclusion would not be valid for a large spill.

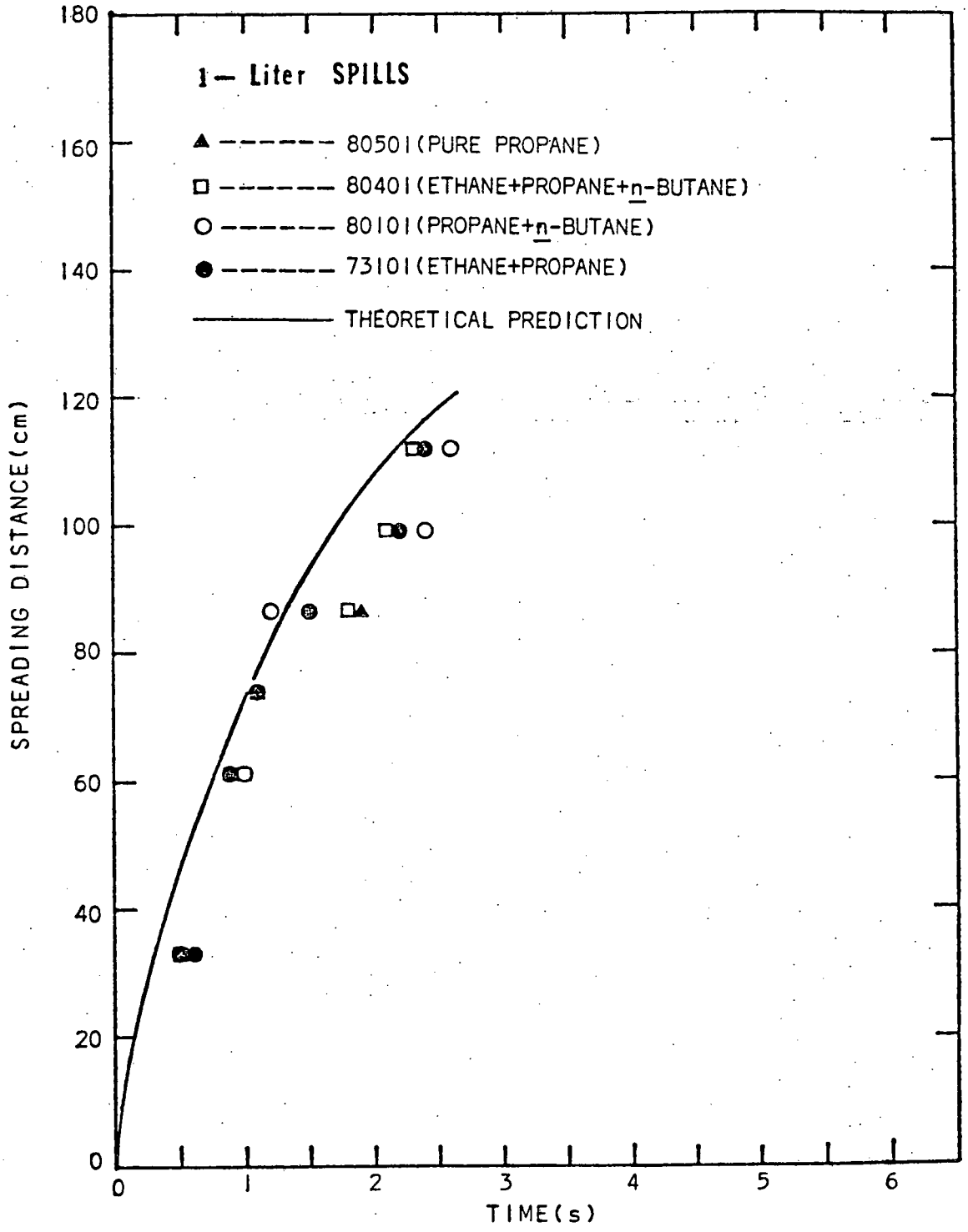

FIGURE I-13: SPREADING CURVES FOR PROPANE AND LPG SPILLS. EXPERIMENTAL DATA AND NUMERICAL PREDICTIONS COMPARED.

TABLE I-3

Maximum Spreading Distance for Propane and LPG Spills

Volume Spilled	Maximum Spreading Distance (cm) Experiment	Theory
0.5 liter	68	79
0.75 liter	90	101
1.0 liter	110	120
1.5 liters	150	153
2.0 liters	163	182

TABLE I-4

*Maximum Spreading Distance for Methane and LPG Spills

Volume Spilles	Maximum Spreading Distance (cm) Methane	LPG
0.5 liter	229	68
0.75 liter	279	90
1.0 liter	317	110
1.5 liters	380**	150
2.0 liters	452**	163

* Experimental Data

** Theoretical Prediction

3. Liquid nitrogen and methane exhibit similar thickness profiles during spreading, that is, the spreading front is thickest and the profile thins out toward the spill origin.

4. The bubbles of evaporated cryogen entrained in the liquid affect the spreading of cryogen on water. The bubbles alter the effective density of the cryogen layer and this effect has been accounted for in the model development.

5. A numerical technique using the method of characteristics has been developed that successfully describes the boiling-spreading phenomena for liquid nitrogen and methane spills on water. The model provides information of the maximum spreading distance and the time for complete vaporization for various quantities spilled.

6. For liquid propane or LPG spills, nucleate boiling occurs upon initial contact with water. Highly irregular ice forms very quickly and the local boil-off rates monotonically decrease with time. A moving boundary heat transfer model can adequately describe the boiling phenomena. This is consistent with earlier observations made for propane or LPG spilled on confined water surfaces.

7. For LPG mixture spills, fractionation occurs with the more volatile components vaporizing preferentially.

8. Addition of small quantities of ethane or n-butane to propane has little effect on the boiling process. This was also the case in confined propane and LPG spills.

9. Propane or LPG does not spread in a manner similar to liquid nitrogen or methane. The formation of a rough ice layer hinders the spreading of propane and LPG and the spreading was found to be linear with respect to time.

10. The composition of LPG has essentially no effect on the spreading phenomena. Pure propane will simulate actual LPG behavior. The same conclusion

was obtained in confined LPG spill experiments.

11. Irregular ice formations in LPG spills are difficult to characterize and their effect on hindering the spreading of LPG cannot be adequately accounted for in the theory. The numerical model does not adequately describe the boiling-spreading phenomena for LPG spills.

12. In an industrial accident, it is expected that LNG will spread over a much larger area than LPG for the same volume spills. In this case, the formation of an ice layer beneath the cryogen may lead to much lower evaporation rates.

12. The high-speed motion picture photographic study improved the understanding of cryogen movements, ice formation and bubble growth in the boiling/spreading process.

The work described in this thesis provides a first step towards estimating the extent of hazardous spills from an LNG or LPG tanker accident.

REFERENCES

Boyle, G.I. and A. Kneebone, "Laboratory Investigations into the Characteristics of LNG Spills on Water. Evaporation, Spreading, and Vapor Dispersion", API Report 6Z32, Shell Research Ltd., Thornton Research Center, Chester, England (1973).

Burgess, D.S., J.N. Murphy and M.G. Zabetakis, "Hazards Associated with the Spillage of LNG on Water", Bureau of Mines Report on Investigations RI-7448, U.S. Dept. of Interior (1970).

Eckert, E.R.G. and R.M. Drake, Analysis of Heat and Mass Transfer, McGraw-Hill, New York (1972).

Fay, J.A., "The Spread of Oil Slicks on a Calm Sea", Oil on the Sea (ed. by D. Hoult), pp. 53-64, Plenum, New York (1969).

Fay, J.A. "Unusual Fire Hazard of LNG Tanker Spills", Combustion Sci. and Tech., 7, 47 (1973).

Hoult, D.P., "Oil Spreading on the Sea", Annual Review of Fluid Mechanics, 4, 341 (1972a).

Hoult, D.P., "The Fire Hazard of LNG Spilled on Water", Proc. Conference on LNG Importation and Safety, Boston, Massachusetts, 87 (1972b).

Muscari, C.C., "The Evolution of Liquid Natural Gas on Water", M.S. Thesis, Massachusetts Institute of Technology, Cambridge, Massachusetts (1974).

Otterman, B., "Analysis of Large LNG Spills on Water — Part I: Liquid Spread and Evaporation", Cryogenics, 15, 455 (1975).

Raj, P., "Simultaneous Boiling and Spreading of LNG on Water," Proposal to GRI, Department of Chem. Eng., Massachusetts Institute of Technology (1978).

Raj, P. and A. Kalelkar, "Fire Hazard Presented by a Spreading Burning Pool of Liquefied Natural Gas on Water", Presented at Combustion Institute (USA) Western Section Meeting (1973).

Reid, R.C. and K.A. Smith, "Behavior of LPG on Water", Hydrocarbon Processing, pp. 117, April (1978).